1

Climate and Environmental Modelling

The C-MMACS Environmental Modelling Programme (CEMP)

Capacity to model and forecast atmospheric, oceanic and environmental processes at user-specified spatio- temporal scales can revolutionize our approach and ability to address many issues that concern us closely. The **C-MMACS Environmental Modelling Programme (CEMP)** is a comprehensive multi-component initiative, comprising modelling of ocean, atmosphere, environmental and climatic processes for a better understanding and enhanced forecast capability.

Over the years, CEMP has slowly grown in its scope and capability. A multi-pronged approach, involving research in process modelling, model evaluation, forecast methodology and alternative modelling has resulted in several milestones in CEMP.

Inside

A Schematic Representation of CEMP

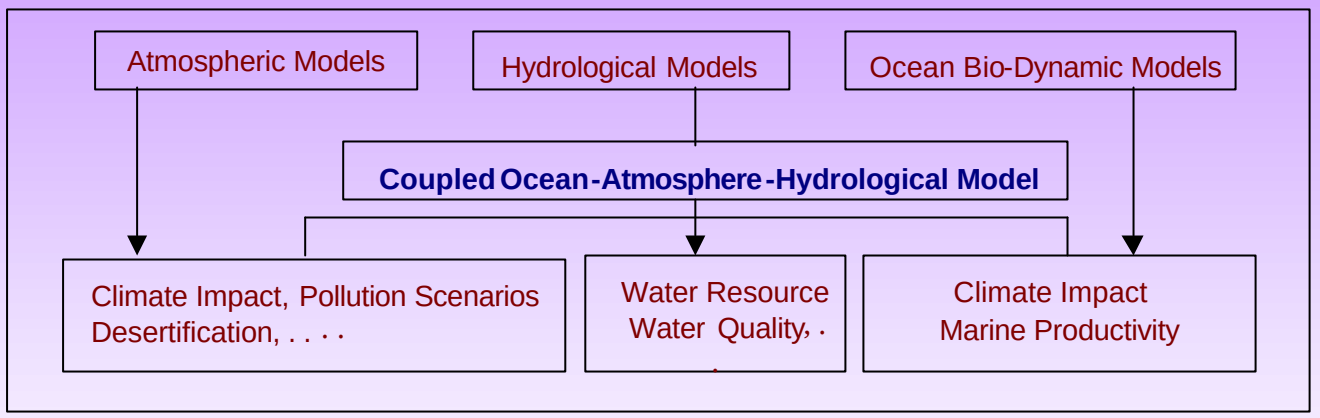

Some Milestones

The Modular Ocean Model has been installed and evaluated; this paves the way for ocean state forecasting.

A comprehensive dynamical mechanism for the broad spectrum of tropical variabilities has been developed; this has direct implications for model improvement and model evaluation.

A new parameterization of convection in the tropics has been developed using the concept of convective time lag.

A preferred scale for intensification of tropical disturbances has been predicted using numerical experiments; this has direct implications for early identification and early warning of tropical cyclones.

Process models for marine primary productivity have been developed and evaluated. This forms the basis for modelling higher trophic levels.

The Neural Network model developed at C-MMACS for long-range forecasting of monsoon rainfall has been successfully used to generate experimental forecasts for the past seven years.

CEMP: Major National and International Collaborations

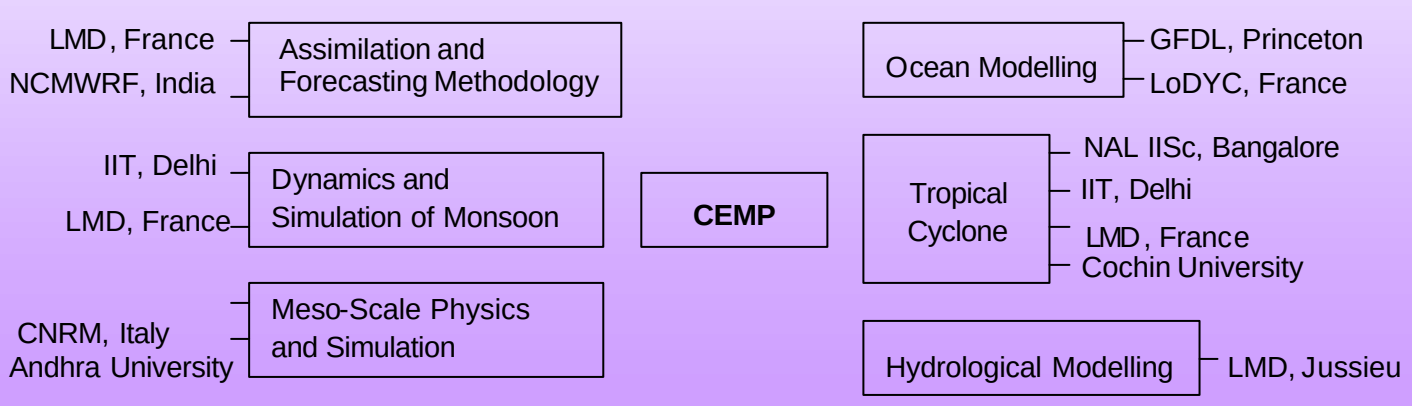

Multi-Method Experimental Forecasts of Summer Monsoon 2003

The experimental forecast system at C-MMACS is aimed at developing and testing methodology for improved range, scope and reliability. The philosophy behind multi-method forecasting is to use forecasts from complimentary forecast methods like dynamical model, neural network and diagnostics method to enhance scope and reliability of the forecast. The neural network forecast method, termed cognitive network, has been used to generate all-India summer monsoon rainfall (ISMR) since 1995. There is, however, urgent need for-improving the scope for the forecast in terms of spatio-temporal scales. In view of this, and the failure of most methods to predict the unusual monsoon of 2002, we have adopted a multi-method approach, combining different methods like neural networks, diagnostic model and dynamical models to improve overall scope and reliability. Here we present experimental forecasts for certain aspects of summer monsoon of 2003.

The best candidate for generating forecasts with high spatio-temporal resolution (preferably at user specified scales) is a dynamical model. As the monsoon is a large scale system, it is necessary to use a global circulation model (GCM) to simulate and forecast monsoon. At the same time, the monsoon dynamics is affected by convective systems which have scales as small as a few kilometers. This makes it necessary to use as high a spatial (and hence temporal, for reasons of numerics) resolution as possible.

We have adopted the version LMDZ.3.3 with a zoom (VR GCM) developed at the Laboratory for Dynamic Meteorology, Paris. The zoom is around 75^0E,15^0N. The highest resolution (near the centre of the zoom) is about 0.5^0 x 0.4^0 in longitude and latitude, which merges uniformly to 2^0 in longitude and 1.25^0 in latitude away from the zoom. The number of vertical levels used is 19. The present version includes a land-surface model and a diurnal cycle. The convection parameterization scheme is that of Tidke.

We have generated long-range frecasts of monsoon of 2003 using the VR GCM with the initial fields from April 1, 2003 from NCEP (National Center for Environmental Prediction) and monthly climatology of SST fields from AMIP (Atmospheric Model Intercomparison Project). Although it is desirable to use multiple initial f\conditions for assessing reliability, the present experimental forecasts are limited to one initial condition. More importantly, a model climatology is required for a meanigful forecast of anomaly fields. In the present case an 11-year model climatology was generated.

1.1 Advance Forecast of Monsoon Onset

The onset of the monsoon, the day of its arrival in Indian main land can be defined in a numer of ways. Keeping in mind the user need and simplicity in terms of observation and interpretation, we define onset as the first sustained large scale (area averaged rainfall lasting 3 days or more) above a threshold (3mm/day) after May 20. We consider two locations: one over the coast of Kerala and the other over the north-east India.

Fig 1.1 shows the time series of area-averaged daily rainfall over Kerala for 2002 and 2003. As per our definition, the monsoon onset over Kerala will be delayed until about June 6. However, there is likely to be an early onset over the north-east India around June 3. These onset forecast were generated using the variable resolution GCM described above. The curve for 2002, which shows timely onset as observed, is included for comparision.

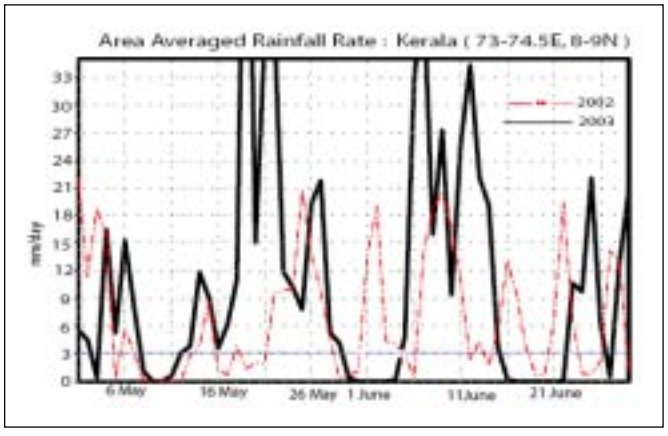

Fig. 1.1 Area-averaged rainfall over Kerala for 2002 and 2003.

The dynamical forecast indicates a late arrival of monsoon in terms of sustained area-averaged rainfall over the coast of Kerala; while there will be a weak onset around June 1, 2003, there will be depression in rainfall until around June 6, 2003.

(P Goswami, A Mandal)

1.2 High-Resolution Advance Forecast of Monthly Rainfall

The structure of the monthly anomaly fields (with respect to 11-year model climatology) of rainfall for June, July and August, 2003 from the VR GCM simulation with initial condition for April 1, 2003 are shown in Fig. 1.2.

For the month of June, there is likely to be above normal rainfall activity over the Southern and north-eastern India with the rest of the country receiving near normal rainfall.

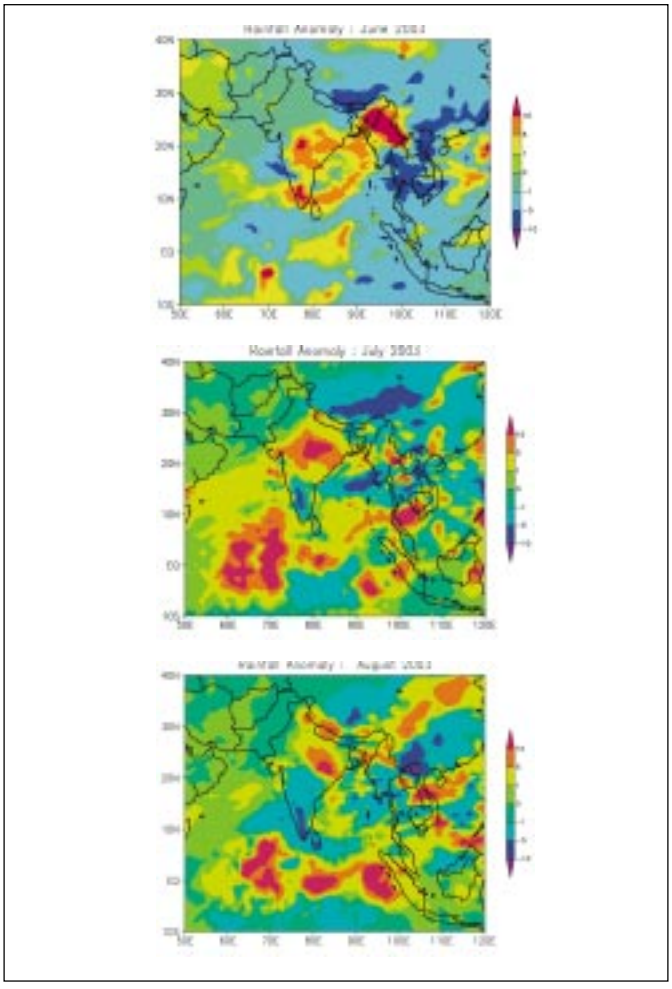

Fig 1.2 Rainfall anomaly for June, July and August 2003 generated with an initial field of April 1 (NCEP) and Climatological SST.

The dynamical forecast for July indicates less than normal rainfall over a large part of South India, especially over Karnataka, and excess rainfall over central and western India, including Gujarat Fig 1.2. Similarly, the experimental forecast for August 2003 shows less than normal rainfall over most part of India.

(P Goswami, A Mandal)

1.3 Neural Network Forecast

The neural network forecast method developed at C-MMACS (cognitive network) has been very successful in generating long-range forecasts of all-Indian summer monsoon rainfall.

Experimental forecasts generated well ahead of the season, and often two seasons in advance, have shown average error less than 4% until 2002; the gross failure in 2002 is clearly visible in Fig 1.3.

The forecast for all India summer monsoon rainfall for 2003, based on this modified algorithm is 740 ± 40 mm which, with respect to a mean of 887 mm, is 15% ± 4% below normal.

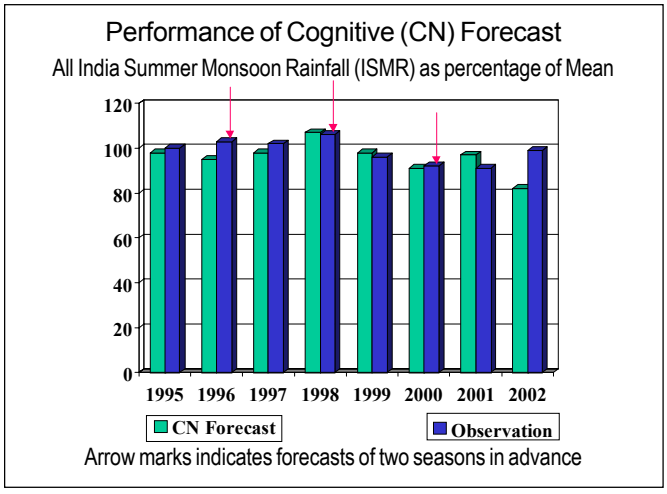

Fig. 1.3 Comparision of experimental forecasts of all-India summer monsoon rainfall using cognitive network with observation. The arrows represent forecasts two seasons in advance.

(P Goswami)

1.4 Characteristic Scale of Convective Organization and Monsoon Performance

The variability of Indian summer monsoon (ISM), including the severe deficit of 2002, appears to strongly associated with convergence organized at a particular scale. Organization is a characteristic feature of atmospheric circulation at all scales, from eddies in the planetary boundary layer to tropical cyclones to mid-latitude depressions, the question of organization is particularly important, and complex, in case of convective systems. In particular, convective forcing in the atmosphere also depends on the organization of the convection. We examine this issue for the specific case of Indian summer monsoon. The variability of the ISM, especially at inter-annual scale, are still poorly understood and hence poorly simulated even by the most advanced models of general circulation (GCM). An analysis of 60-years of NCEP data shows that strength of organized convergence over a scale of about 20^0 around south India (75^0E, 100^0N). In particular, the year 2002 was characterized by very pronounced suppression of this organized convergence. Significantly, the critical location is the (maritime) Southern India and not northern India, which implies that the organized convergence over South India works like a pump to collect the required moisture to fuel the monsoon engine. Our analysis explains a large part of inter-annual variability of ISM and also indicates a lower than normal monsoon for 2003.

The ISM is among the most complex atmospheric systems; difficulties in simulating and forecasting monsoon rainfall have been well recognized. A particularly pertinent example is the case of ISM of 2002, which was predicted to be (near) normal by most forecasting efforts, using methodology

ISM is a large-scale convective system. While the surface heat source that develops due to the seasonal cycle of solar heating initiates the low-level convergence, development of a deep heat source through moist convection is necessary for large-scale precipitation. A well-known effect in tropical dynamics is convective feedback, leading to scale selection. A consistent and comprehensive theory of scale selection in tropical circulation was provided by Goswami and Rao and Goswami and Mathew introducing the concept of a convective feedback. Dynamically, the situation is akin to a conditional instability of second kind, where a weak perturbation (low-pressure system) can amplify by inducing convergence over a wide domain. If the converging air is moist (conditional instability), the response will be an upward transport of moist air through the induced secondary circulation, and consequent precipitational heating leading to further intensification (until non-linear saturation). Implicit in the above dynamical scenario is a characteristic scale over which such organization must take place for the system to develop. The purpose of the present work is to show that such a characteristic scale of convergence indeed exists for ISM, and to quantify this scale, using long-period data from NCEP Reanalysis.

We characterize and quantify convective organization through the quantity

$$C_{LS} = \frac{1}{s}\int_{S}\int_{z=H_1}^{H_2}\left(\frac{\partial u}{\partial x}+\frac{\partial v}{\partial y}\right)dzds$$

Where S represents the scale (radius) over which the convective organization is considered, and H1 and H2 are the lower and upper limits, respectively, for vertical integration.

Numerically, C_{LS} is computed by considering appropriate longitudes and latitudes to represent a circular domain of radius R_0. As the NCEP Reanalysis used here has a resolution of 2.5^0x2.5^0 in longitude and latitude, the smallest step by which R_0 can change is about 250kms. H_1 and H_2 correspond to 1000 and 500 mb, respectively.

To associate C_{LS} and rainfall, the 55 years (1948-2002) of NCEP reanalysis were categorized as excess; normal and deficit years based on the area averaged seasonal (June-September) precipitation over a rectangular box (70^0E-85^0E; 10^0N-30^0N). An (non-dimensional) index for ISM is then defined by

$$R_N = \frac{R_i - \overline{R}}{\sigma}$$

Where R_i is ISM rainfall for the year i, $\overline{R}$ is mean (100-year) ISM rainfall and σ, the standard deviation.

A year is categorized as excess, normal or deficit depending upon the value of R_N

$$R_N \begin{cases} > 0 & : \text{Excess} \\ < 0 & : \text{Deficit} \\ \text{Otherwise} & \text{normal} \end{cases}$$

Table 1: Association of organized convergence at different scales with monsoon rainfall

	α at scale S=			
Location (long-latitude)	10^0	20^0	30^0	40^0
North India (80^0E, 15^0N)	2.5	5.4	-8.4	-1.5
South India (80^0E, 5^0N)	-0.5	7.9	12.0	5.6
East India (85^0E, 15^0N)	6.9	3.4	-11.0	-2.3
West India (75^0E, 15^0N)	-18.0	-5.0	-3.2	-0.3

To examine the contrast between the low–level convergence field for excess and deficit rainfall years, we first construct climatology of the convergence field for excess years as follows.

$$\overline{C}_{LSE}(i) = \frac{1}{N}\sum_{n=1}^{N_E} C_{LS}(n,i,n), i = 1,....150$$

Where, n represents the year and i represent time in days with day 1 corresponding to May 1 of the corresponding year. The climatology of C_{LS} for deficit years (C_{LSD}) is constructed in a similar fashion.

To bring out clearly the difference between excess and deficit years in terms of low-level convergence, we further define the quantities:

$$\Delta C_{LS}(m) = \overline{C}_{LSE} - \overline{C}_{LSD}$$
$$\Delta R_A(m) = \overline{C}_{AE} - \overline{C}_{AD}$$

Where C_{LSE}(C_{LSD}) represents the daily climatology of C_{LS} over the excess (deficit) years.

The corresponding climatologies of area averaged precipitation are created in a similar fashion:

$$\overline{R}_A(i) = \frac{1}{N}\sum_{n=1}^{N} R_R(i,n)$$

Where N is the number of excess or deficit year as the case may be R_A is the area averaged daily precipitation rate.

To determine the scale and location at which convective organization is most strongly associated with large-scale precipitation we consider four locations and four scales centered at each of these locations, as given in Table 1. The table shows the organized low-level convergence (considered positive) integrated over the period June1 - Sep30. The scale of 20^0 south India has the most consistent positive signal. For subsequent discussion, therefore, we shall only consider the location over south India at 20^0 scale. As the centre is over 5^0N, this will cover up to 15^0N. Figure 2 shows the difference in daily climatologies of convergence (treated as positive) for excess (C_{LE}) and deficit (C_{LD}).

The results are shown for three values of radius of convective organization for each of the four locations as indicated. The numbers in brackets in each panel represents the mean of the 150 values for the corresponding case. A very clear signal is evident for $S=20^0$ over each of the regions except West India. On the other hand, no clear or consistent signal exists for the other values of S. To begin with, for $S=20^0$ over south India the quantity ΔC_{LS} is mostly positive beyond day 60 (i.e. for July-September period) indicating that the excess years have stronger convergence than the deficit years in general. Similar conclusions also hold for two other locations i.e, North India and East India, for both $S=10^0$ and $S=20^0$. Over West India however, the trend is somewhat reversed, with deficit years showing stronger convergence. More dramatic, however, is the structure of CLS at $S=40^0$ (dash line) which is close to zero and shows no definite trend over all the four locations. In other words, a clear contrast between excess and deficit years exists only in low-level convergence organized at specific scales i.e, 10-20^0.

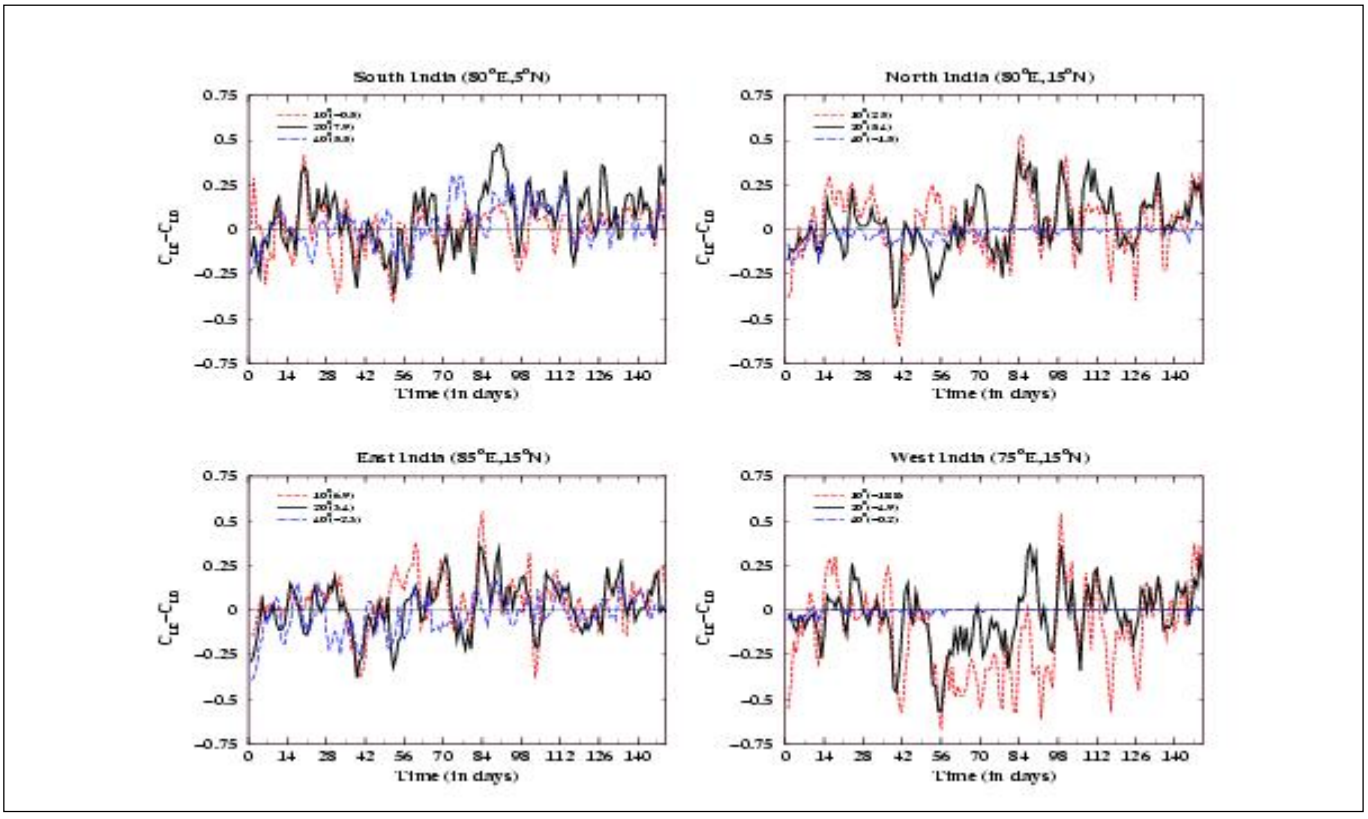

Fig. 1.4 Contrast between daily values of low-level convergence organized over different scales for excess and deficit monsoon years. Each curve represents difference in daily low-level convergence averages over excess (C_{LE}) and deficit (C_{LD}) years. Divergence value has been excluded for convenience of interpretation. The numbers in brackets for each scale indicates the sum of low-level convergence at that scale for the June 1 to Sept. 30 period, in the figure day 0 corresponds to May 1.

Fig 1.5 brings out the association between C_{LS} and rainfall clearly, which compares the quantity ΔC_{LS} for 20^0 with the corresponding quantity ΔR, defined similarly.

It is worth noting that the quantity ΔC_L, for the most part of June; a higher than normal rainfall in June can be often a herald of subsequent deficit. Another significant feature is the significant positive value of ΔC_L in the second half of May.

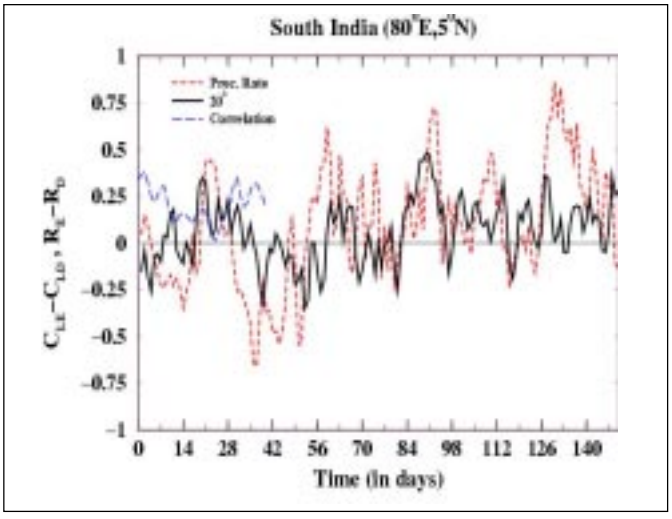

Fig. 1.5 Association between contrast in daily precipitation (short-dashline) averaged over excess and deficit monsoon years and corresponding values for low-level convergence organized at 200 scale (thick solid line). The long-dash line shows correlation between the two at different lags. A notable feature in the general excess of low-level convergence as well as daily rainfall for the excess

The other interesting feature that contrast is more pronounced for the centre over south India. Although this may appear counter-intuitive at first sight, it needs to be recalled that a necessary condition for monsoon precipitation is an adequate supply of moisture. The above result indicates that it is the south Indian centre that, working as a pump through low-level convergence, supplies the necessary moisture to the continental India. The North-Indian centre of organized convection then lifts this moisture to bring about the monsoon precipitation.

(P Goswami, G K Patra)

1.5 Modelling of Biogeochemical Cycles

The growth of phytoplankton in open seas and neritic waters over continental shelf often depends on the nitrogenous nutrient, which is available in several forms. Nitrate is brought into the mixed layer from deeper regions by the processes of upwelling, entrainment, mixing and advection. Ammonium and nitrite are produced locally by biological processes involving zooplankton and bacteria. The uptake of the former inorganic form of nitrogen is associated with new production and it has been studied extensively following intense interest in determining the role of marine biological processes in the carbon cycle, and hence in global warming. While the uptake of each nitrogenous nutrient depends on its concentration according to Michaelis-Menten relation, ammonium is well known to suppress the uptake of nitrate. The mechanism of this nutrient interaction is explained in terms of cell physiology. The inhibitory effect of ammonium on nitrate uptake can be viewed as a particular case of the uptake of nutrients by phytoplankton in a multi-nutrient environment with possible nutrient interaction.

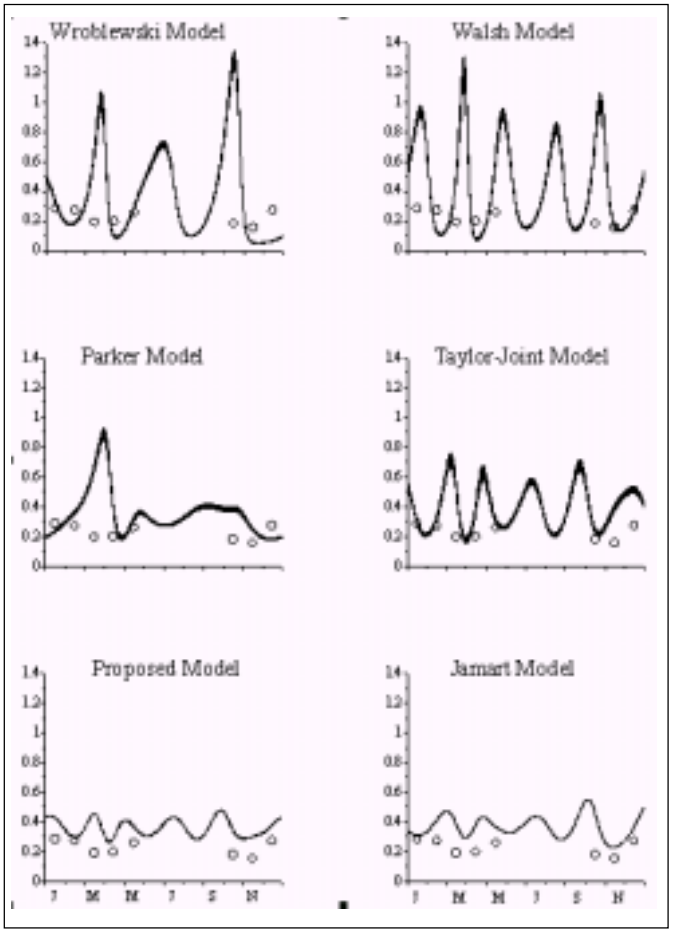

Fig. 1.6 Comparison of the seasonal variation of chlorophyll obtained from different model simulations with the monthly average values of chlorophyll from the SeaWiFS data for the year 2000.

Five different relationship have been proposed for the inhibition of nitrate uptake by ammonium. Only two relationship have found significant acceptance in marine ecosystem simulations. The new formulation proposed for uptake of nutrients in a multi-nutrient environment is phenomenological in character with similarity and hyperbolicity taken as basic properties. When it is applied

to the nitrate-ammonium environment in Arabian Sea, the results are found to agree well with the recent observations. The generality of the framework offers possibilities of applications to other multi-nutrient environments.

All the six two nutrient interaction relationship have been introduced into the seven component marine ecosystem model to study the effect of this formulation on the behaviour of the biogeochemical variables in the mixed layer. The model simulations were carried out using the parameters from literature. The seasonal variation of chlorophyll obtained from different model simulations were compared with the monthly average values of chlorophyll from the SeaWiFS data at several stations in Arabian Sea and Bay of Bengal.

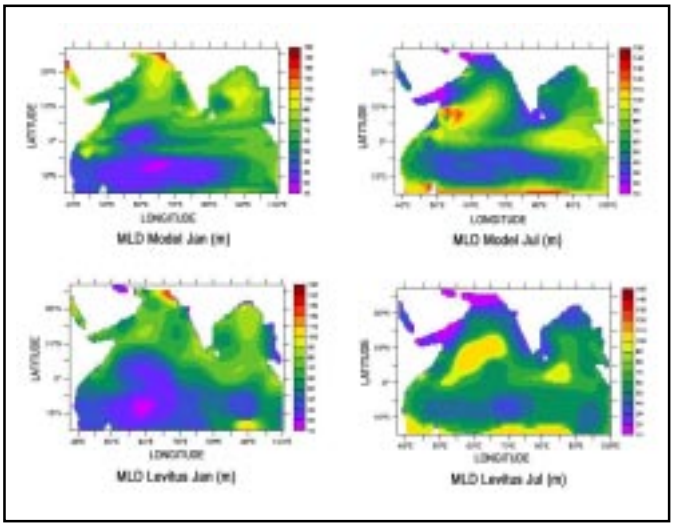

Fig. 1.7 Mixed layer depth distribution in the North Indian Ocean: Comparison of physical model simulation with Levitus atlas for January and July. The deep mixing in January in the northern Arabian Sea is due to winter cooling and that in July is due to evaporative cooling during SW monsoon.

It was found that the model simulations with the new formulation gave better comparison with the data (Fig.1.6). Seasonal variation of different variables and fluxes for all the formulations were studied to understand the effect of different formulations of the ammonium inhibition of the nitrate uptake by phytoplankton on the marine ecosystem dynamics. The question of the nature of effects of inaccuracies in the representation of interaction of ammonium and nitrate uptake on the dynamics of the marine ecosystem was also addressed by considering the effect of the interaction on the f ratio, which is defined as the ratio of the new primary production to the total primary production (Details are given in RR 0201).

An investigation is presently underway at C-MMACS on the effects of various representations of nutrient interaction on the simulations of marine ecosystem in the Indian Ocean with a three-dimensional physical oceanographic model (MOM) coupled with a biological model (FDM). The simulations were performed for three kinetic relationship of uptake namely, Wroblewski, 1977; O'Neill et al., 1989; Yajnik & Sharada, 2002, using climatological forcings. The values of kinetic parameters were determined from the experiments of McCarthy et al (1999).

The mixed layer depths (MLD) from the model and the Levitus atlas (1994) show very good agreement (to within 20 m in most places) in January, while the agreement in July off the Somali coast is not as good, possibly due to strong winds (Fig.1.7). The temporal variation of salinity with depth calculated by the model, at four locations, two each in

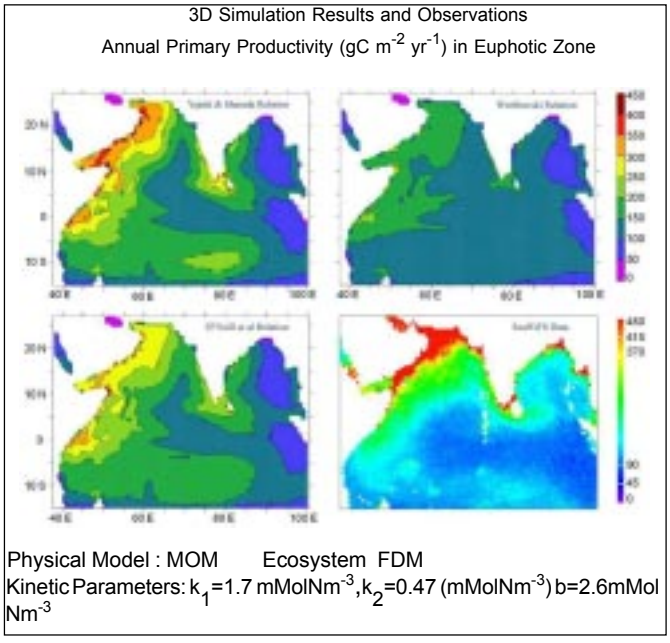

Fig. 1.8 : Annual average primary productivity in the North Indian Ocean: Comparison of 3D model simulations with three different kinetic relations for the uptake by phytoplankton (Wroblewski, O'Neill et al and Yajnik & Sharada) with SeaWiFS derived values.

Arabian Sea and Bay of Bengal, shows that the salinity in Bay of Bengal is much lower than that in Arabian Sea, during all the seasons. Salinity is highest in Arabian Sea during summer and south-west monsoon seasons because of high evaporation. Salinity is lowest in Bay of Bengal after the SW monsoon because of the river runoff. The spatial variation of annual average primary productivity, especially in the regions of high primary productivity in the northern Indian Ocean, is found to agree most favourably with SeaWiFS data for the relation (Yajnik & Sharada, 2002) based on similarity and hyperbolicity (Fig.1.8). The distribution of particle export ratios also appears to be close to current expectations. The profiles at JGOFS station S4

(19^{0}N, 59^{0}E) obtained from the three simulations were compared with those obtained from JGOFS cruise data. Fig. 1.9 shows the profiles for nitrate concentrations at six times in a year. Clearly, Wroblewski relation gives the largest departures from what is observed and the new proposed relation gives the smallest.

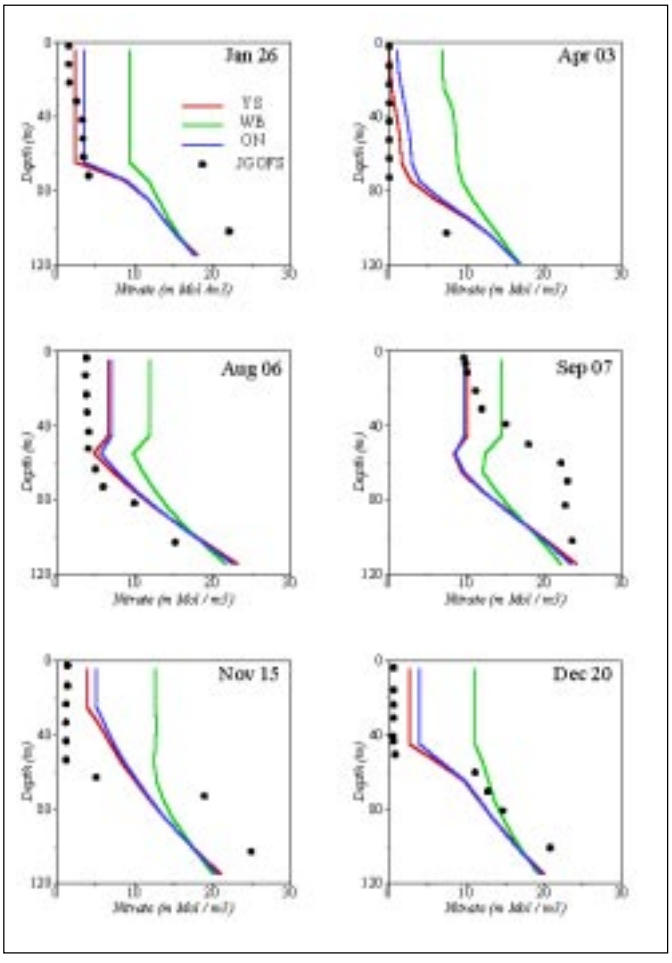

Fig. 1.9 : Seasonal variation of nitrate profiles at 19^{0}N, 59^{0}E: Comparison of results of three simulations (Kinetic relations of Wroblewski (WR), O'Neill et al (ON) and the proposed relation (YS)) with JGOFS data.

Since the simulation results were highly sensitive to the parameter values used in the ammonium inhibition relations, some optimization schemes are being applied to get the parameter values leading to more realistic simulation results. (Details are given in TM 0201).

(M K Sharada, K S Yajnik and P Swathi)

1.6 Geostrophic Current Computations of the North Indian Ocean

As a part of this we have used various sources of observations for computing the geostrophic currents of the

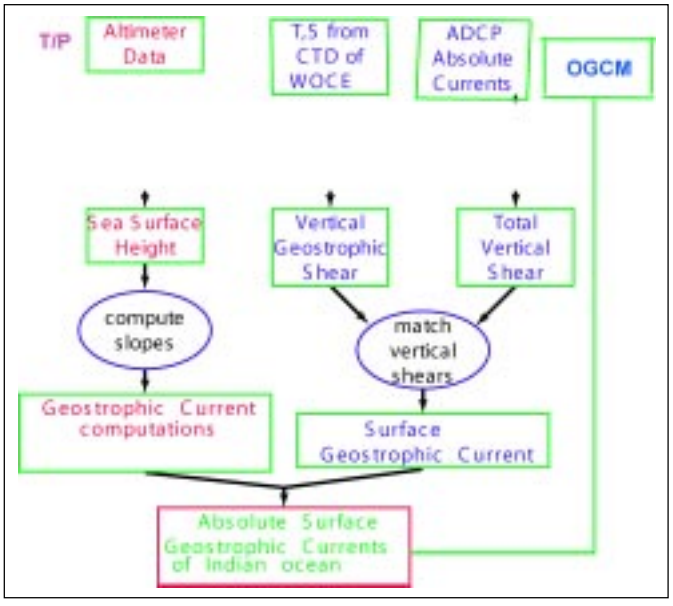

Fig. 1.10 Schematic representation of Geostrophic current computations using data from various available resources and comparison with model simulations for the Indian Ocean.

North Indian Ocean. The aim of this work is to analyse various datasets to bring out a climatological current dataset for validation purposes. We have used Topex Poseidon altimeter derived sea surface height. The SSH has been regridded to 1.5^o x 1^o latitude x longitude. The SSH has been analysed in detail for studying the various circulation features of the Indian (PDCM 0207).

This SSH has been used to compute geostrophic currents of the North Indian Ocean for the years 1994-1999. Also we have used the temperature and salinity profiles of US JGOFS and Indian JGOFS programs and computed the currents. Along with this we have analysed the ADCP observations which are available as a part of the WOCE program. The schematic picture of geostrophic current computations of the Indian Ocean is shown in Fig.1.10.

(C Kalyani Devasena and P S Swathi)

1.7 Comparison of Temperature and Salinity Profiles of the Model Simulations and Observations

We have made various simulations with MOM (Modular Ocean Model) using different wind stresses to study the thermal structure and mixed layer variations of the Indian Ocean. The model domain is 37.6^{o}E-100^{o}E with a resolution of 0.4^o. The latitudinal extent is from 15^{o}S-27.4^o N with a resolution varying from 1^o at 15^o S to 0.4^o north of the equator. There are 35 vertical levels (10m in upper 100 m, 20 levels in top 300 m and 35 levels to a full depth of 5600m).

The increased resolution in the top few hundred meters is for simulating thermal structure and heat content of the mixed layer better. We have taken monthly fluxes from a 50 year run as input to our model.

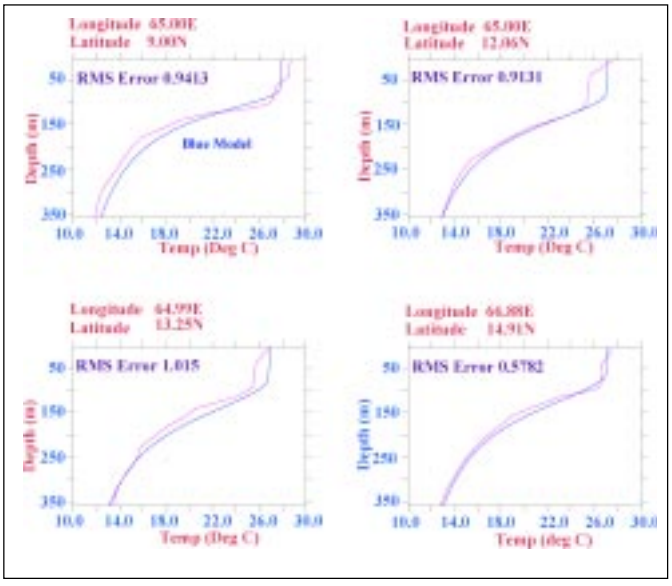

Fig. 1.11 Comparison of model simulated temperature profiles with US JGOFS observations at a few locations (transect39) in September.

The temperature and salinity profiles of the model simulations were compared with observations along the available transects of US JGOFS and Indian JGOFS for various latitude and longitude points. Fig. 1.11 shows the temperature profiles of the model versus observations along with RMS error for a few locations along the US JGOFS transect 39 during September, whereas Fig. 1.13 is for salinity.

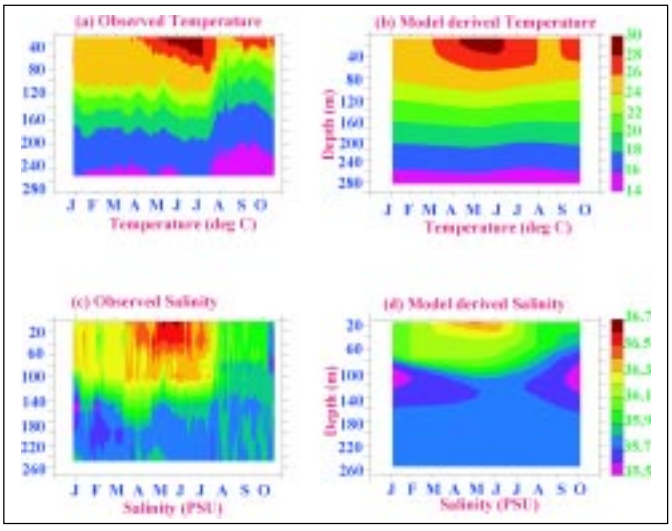

Fig. 1.12 Comparison of model derived temperature (Top Right panels) for the year 1995 with the temperature (Top left panels)observed at the Moored Buoy site in the Arabian Sea (Buoy data courtesy Albert Sok Fischer and Bob Weller) and Model derived salinity profiles (bottom right panels) with observed salinity (bottom right) of the buoy site (location of the buoy site is 61.5^{O}E longitude and 15.5^{O}N latitude).

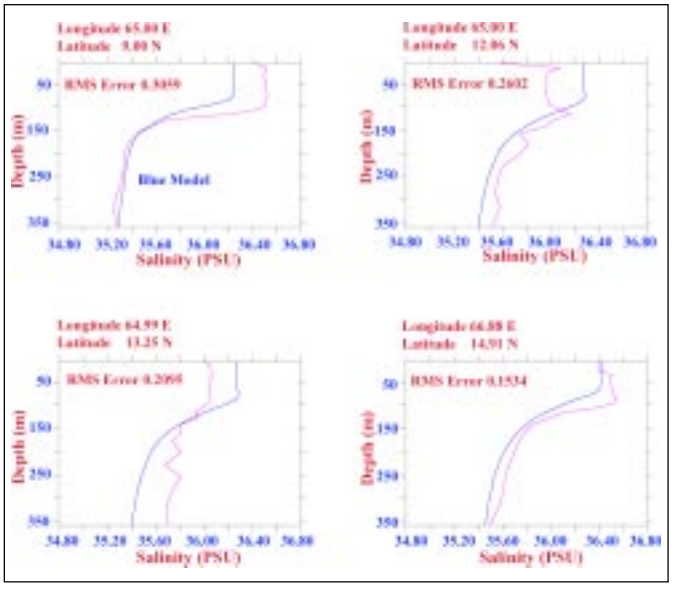

Fig. 1.13 Comparison of model simulated salinity profiles with US JGOFS observations at a few locations for the transect39.

We have also compared the model simulated temperature and salinity with available time series observations of the moored buoy (1 year). The model (Fig. 1.12) is able to capture the mean distribution very well but not able to pick-up the small scale features which were seen in the observations. This is to be expected as the model is forced with smooth climatological winds. The observations available as a part of the Indian JGOFS are also used for comparing the salinity and temperature profiles of the Indian Ocean with model simulations.

(C Kalyani Devasena and P S Swathi)

1.8 Construction of SST Field from Simulated Sub-surface Temperature

The objective of the present work of SST reconstruction is two-fold: first we propose and evaluate a simple process model to construct the SST field from the given field of sub-surface temperature and low level wind. Secondly, by taking the low-level wind from the daily fields of surface wind from NCEP data and the sub-surface temperature from an OGCM simulation, an evaluation of the OGCM as a component for a CGCM is carried out.

The SST field in general is a complex function of atmospheric and oceanic variables. Our objective is to explore and evaluate a relatively simple process model for constructing the SST field from the given field of sub-surface temperature(T_5) and low-level wind as follows

$$T_c = T_5 + \beta\,(T_5 - T_{min})W_L + \gamma\, W_L\,(T_c - T^*)$$

Typically in a CGCM, T_5 would come from the temperature simulated by the ocean model at the first level below the surface, while W_L would represent the wind field simulated by the atmospheric component at the lowest model level. A variable β is used as

$$\beta = \begin{cases} 0.2 & W_L > U_{crit} \\ 0.1 & \text{otherwise} \end{cases}$$

where U_{crit} is the critical velocity, which is taken as 5m/s. In the present work we compute W_L from the daily data of surface wind components from NCEP data sets while T_5 is taken as temperature field at 5m level simulated by an OGCM.

The quantity $\gamma\, W_L\,(T_c - T^*)$ represents the quantity of evaporative cooling. T* is a threshold for SST below which this term is not in effect. T* is taken as 28° Celsius. A correction factor is included in the second term using a minimum value of T_5 denoted by T_{min} over the whole year.

We have used version 3 of Modular Ocean Model (MOM) developed at GFDL, Princeton. MOM describes the 3-dimensional dynamics of the global ocean circulation with realistic coastlines with various options for mixing schemes. The basic formulation of the model has been described in many studies (Bryan, K and M. D. Cox, JPO 1972, 510-514) and here we shall highlight only a few points that needs special attention.

The mixing schemes used are horizontal Laplacian with iso-neutral mixing and K-profile parameterization (KPP) for vertical mixing. Scripps 1° topography is used to define bottom topography. The simulations were carried out on a uniform horizontal grid of 2° in longitudinal direction with 13 vertical levels; the level nearest to the surface is at 5m depth. The latitudinal grid spacing is 0.5° at equator, increasing towards poles with 3° at both poles. The model has a time step of 2 hours for tracers. This is initialized with Levitus climatology for salinity and temperature, the forcing surface boundary conditions are derived from daily NCEP wind field. Wind stress is calculated using speed-dependant drag coefficient. A spin-up period of 5 years was allowed for the model to achieve dynamic equilibrium. Sea Surface Temperature(SST) from available data is used as a restoring force in the model. The model is tested by restoring with different climatological data sets (Reynolds, NCEP, AMIP etc) and with different frequencies(daily, weekly, monthly). The simulation results shows the effects are marginal. The current experiment is using the daily SST climatology from NCEP(T_o)

Several statistical parameters are analysed for the daily values of T_5, T_c and T_o. The aim is to get the best estimate of T_c which gives best results in the analysis. Correlation, absolute error, bias between T_c and T_o as well as between T_5 and T_o, Power Spectral Density (PSD) distribution and Standard Deviation (SD) of T_5, T_c and To are discussed. The latitude-longitude distribution of these parameters are restricted to tropical ocean.

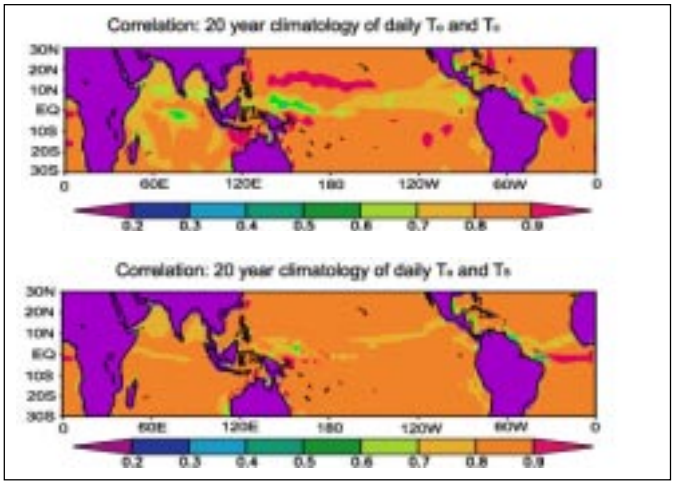

Fig 1.14 Longitude-latitude distribution of correlation coefficient between 20 year climatology of T_o and T_c, and the corresponding distribution of T_o and T_5

The longitude-latitude distribution of correlation coefficient between 20 year climatology of daily T_o and T_c, in Fig 1.14, shows significant correlation over most of the global ocean. There remains, however, a narrow strip around the equator over which the correlation is relatively small.

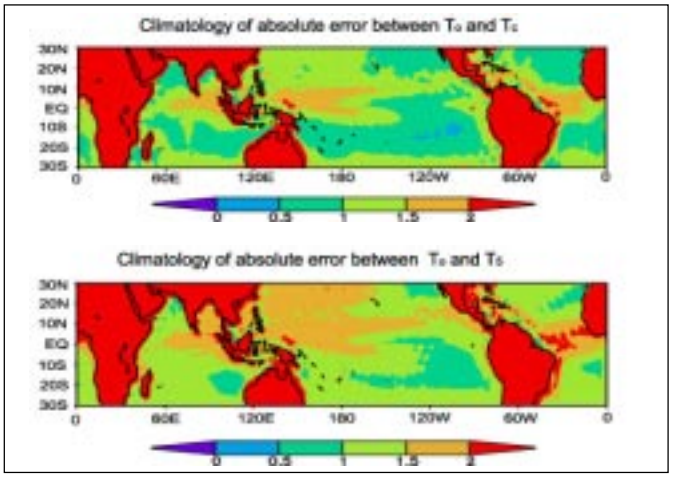

Fig 1.15 Longitude-latitude distribution of absolute error between daily T_c and T_o (mean over 365 days, 20 years) The corresponding structure of error between observed T_o and T_5 shows the improvement due to the inclusion of the correcting factors.

The longitude-latitude distribution of absolute error between T_c and T_o (mean over 365 days and 20 years) is shown in the Fig 1.15. The corresponding structure of mean error between observed T_o and T_5 shows the improvement due to the inclusion of the correcting factors. In particular there is significant improvement over equatorial region.

An important issue in simulation of SST is it's temporal variability. It is now recognized that short-term (intra-seasonal) oceanic variability play important roles in genesis and dynamics of atmospheric variability. An important requirement for the simulated SST , therefore is accurate temporal variability. Fig 1.16 shows the latitude-longitude distribution of 20-year climatology of Standard Deviation(SD) of daily values of T_c, T_5 and T_o. It is clear that sub-surface temperature exhibits far less variability than observed; the constructed SST on the other hand shows Standard Deviation (SD) closer to the observed.

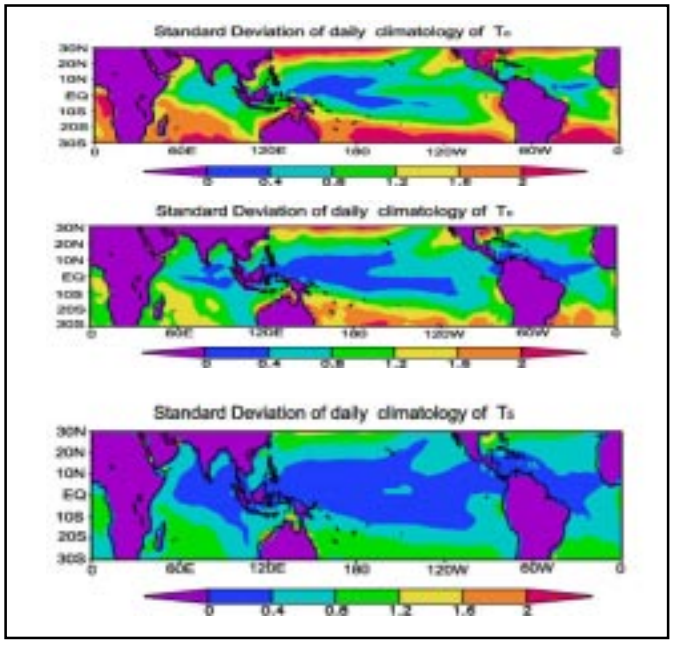

Fig 1.16 Standard deviation(SD): Climatology of daily T_c, T_5 and T_o

The analysis of 20-year climatology of SST constructed from MOM simulations shows that the process model proposed is quite successful in constructing both the amplitude as well as the variability of SST at different spatio-temporal scales. While these results indirectly verifies the MOM simulation, they also bring out the need for accurate simulations of the atmospheric wind field for appropriate simulation of the SST field. Besides, our results imply that given accurate simulation of low level wind field, an OGCM like MOM can be successfully used to derive the SST field in a coupled ocean – atmosphere model.

(P Goswami and P Rajeevan)